

Tomography and spectroscopy as quantum computations

César Miquel¹, Juan Pablo Paz¹, Marcos Saraceno²,

Emmanuel Knill³, Raymond Laflamme⁴ and Camille Negrevergne³

¹ *Departamento de Física, FCEN, UBA, Pabellón 1, Ciudad Universitaria, 1428 Buenos Aires, Argentina*

² *Unidad de Actividad Física, Tandár, CNEA Buenos Aires, Argentina*

³ *Los Alamos National Laboratory, MS B288, Los Alamos, NM 87545*

⁴ *Los Alamos National Laboratory, MS B265, Los Alamos, NM 87545*

Determining the state of a system and measuring properties of its evolution are two of the most important tasks a physicist faces. For the first purpose one can use tomography,¹ a method that after subjecting the system to a number of experiments determines all independent elements of the density matrix. For the second task, one can resort to spectroscopy, a set of techniques used to determine the spectrum of eigenvalues of the evolution operator. In this letter, we show that tomography and spectroscopy can be naturally interpreted as dual forms of quantum computation. We show how to adapt the simplest case of the well-known phase estimation quantum algorithm to perform both tasks, giving it a natural interpretation as a simulated scattering experiment. We show how this algorithm can be used to implement an interesting form of tomography by performing a direct measurement of the Wigner function (a phase space distribution) of a quantum system. We present results of such measurements performed on a system of three qubits using liquid state NMR quantum computation techniques in a sample of trichloroethylene. Remarkable analogies with other experiments are discussed.

The basic idea discussed in this letter can be described in terms of the quantum algorithm represented by the circuit shown in Figure 1 (see [2] for an introduction to quantum circuits and algorithms): A system, initially in the state ρ , is brought in contact with an ancillary qubit prepared in the state $|0\rangle$. This ancilla acts as a “probe particle” in a scattering experiment. The algorithm is: i) Apply an Hadamard transform to

the ancillary qubit (where $H|0\rangle = (|0\rangle + |1\rangle)/\sqrt{2}$, $H|1\rangle = (|0\rangle - |1\rangle)/\sqrt{2}$), ii) Apply a “controlled- U ” operator (does nothing if the state of the ancilla is $|0\rangle$ but applies U to the system if the ancilla is in state $|1\rangle$), iii) Apply another Hadamard gate to the ancilla and perform a *weak* measurement on this qubit detecting its polarization (i.e., measuring the expectation values of Pauli operators σ_z and σ_x). The above circuit has the following remarkable property:

$$\langle\sigma_z\rangle = \text{Re}[\text{Tr}(U\rho)], \quad \langle\sigma_x\rangle = -\text{Im}[\text{Tr}(U\rho)]. \quad (1)$$

Thus, the final polarization measurement reveals a property determined both by the initial state ρ and the unitary operator U . Versions of the above idea play an important role in many quantum algorithms. For pure input states, it occurs in Kitaev’s solution to the Abelian stabilizer problem (a generalization of the factoring problem).³ This was adapted by Cleve *et al.*⁴ to revisit most quantum algorithms, with the circuit of Figure 1 being the simplest instance (see [5] for yet another presentation of the algorithm as a tool for physics simulations). The extension to mixed states and a version of Equation 1 is in [6].

Here, we observe that as a result of Equation 1, this circuit can be used for dual purposes: We can use it to extract information on the operator U if we know the state ρ . Alternatively, we can use it to learn about the state ρ by using some specific operators for U . In this sense, this circuit can be adapted either as a tomographer or as a spectrometer which, therefore, are dual faces of this quantum computation. Moreover, it is interesting to think of the above algorithm as simulating a scattering experiment: The ancillary qubit plays the role of a probe particle: it interacts with the scatterer (the system, initially in state ρ) and is later detected. From the statistics gathered by the detector measuring the polarization of the probe, we can either reconstruct the state of the scatterer (if we know about the interaction) or learn about the interaction (if we know about the state of the scatterer). Describing the algorithm in physics language helps in establishing analogies between the above proposal and some already performed experiments that, interestingly enough, can be interpreted as special instances of the algorithm (see below).

Let us first discuss how to use this to build a spectrometer. The idea is simple: For example, preparing the system in a completely mixed initial state with $\rho = I/N$ (N is the dimensionality of the space of states of the system), the final measurement is $\langle\sigma_z\rangle = \text{Re}[\text{Tr}(U)]/N$. This is directly proportional to the trace of U , the sum of all its eigenvalues, and therefore has information about the spectrum. Moreover, we can build a real spectrometer by simply adding an extra register (with n_1 qubits) and a controlled

Fourier transform. With this new circuit, shown in Figure 2, the final polarization is $\langle \sigma_z \rangle = g(2E) = \text{Re}[\sum_t^T \exp(4\pi iEt/T) \text{Tr}(U^t)]/NT$ (where $T = 2^{n_1} - 1$). The function $g(E)$ is the Fourier transform of $\text{Tr}(U^t)$, which is nothing but the spectral density of U (smoothed over a scale $2\pi/T$). One can use this same idea to design circuits to measure, for example, the structure function, defined as the Fourier transform of $|\text{Tr}U^t|^2$, characterizing the spectral correlations and the level spacing statistics of U , which are of interest in studies of quantum chaos⁷ (some other related constructions and efficient networks can be found in [8]). It is also important to notice that the above is a rather general spectrometer since it can be adapted to study properties of non-Unitary operators. For example, by adding an extra ancillary register one can use it as a spectrometer for any operator obtained as a weighted sum of unitary operators. We emphasize that the above is a *simulation* of a spectrometer where one has complete control over the operator U that acts on the system. This is the case for any physics simulation, either quantum or classical, where our simulation is intended to be used for the purpose of exploring models. On classical computers, the task of providing spectral information as accomplished by this quantum algorithm appears to be exponentially hard in general. Of course, complete determination of the spectrum of U is still inefficient, unless the eigenvalues are hugely degenerate. But using our simulated spectrometer one can efficiently determine important specific properties of the spectrum, such as directly sampling the spectral density or the structure function.

The circuit in Figure 1 can be adapted for another important purpose: state tomography. Every time we run the algorithm for a known operator U , we extract information about the state ρ . Doing so for a complete basis of operators $\{A(\alpha), \alpha = 1, \dots, N^2 - 1\}$ one gets complete information and determines the full density matrix. Different tomographic schemes are characterized by the basis of operators $A(\alpha)$ one uses. In NMR spectroscopy, for example, a convenient basis set is formed by all tensor products of Pauli operators (the basis of the product operator expansion⁹). This kind of tomography is particularly well suited in this context since all $A(\alpha)$ are easily reached from observables by a sequence of r.f. pulses and periods of free evolution.¹⁰ However, as the above is a generic tomographer one can explore other choices. In particular, we can use it to implement another important tomographic scheme characterized by the operators

$$A(q, p) = \frac{1}{2N} \tilde{U}^q R \tilde{V}^{-p} \exp(i2\pi pq/2N), \quad (2)$$

where \tilde{U} is the operator producing a cyclic shift in the computational basis ($\tilde{U}|q\rangle = |q+1\rangle$), \tilde{V} is the shift in the basis related to the computational one via the discrete Fourier transform and R is the reflection operator

$(R|q\rangle = |N - q\rangle)$. By doing this, we measure the discrete Wigner function of the state of the system, which is defined as $W(\alpha) = \text{Tr}(A(\alpha)\rho)$ (we use $\alpha = (q, p)$). This function is the basic tool to represent the state of a quantum system in phase space, the natural arena of classical physics¹¹ and has often been used to understand the nature of the quantum to classical transition.¹² Its use is common in various areas of physics, but has been mostly restricted to continuous systems (discrete Wigner functions have been used only recently in the context of quantum computation¹³). The defining properties of the Wigner function are: (P1) $W(\alpha)$ is real valued, (P2) Inner products between states ρ_1 and ρ_2 can be obtained as $\text{Tr}(\rho_1\rho_2) = N \sum_{\alpha} W_1(\alpha)W_2(\alpha)$, (P3) Adding the value of $W(\alpha)$ over all points in any phase space line gives a positive number which is the probability of measuring a physical observable. These are consequences of interesting properties of the phase space point operators $A(\alpha)$.^{13,14} One of these properties is the completeness of the set $A(\alpha)$ (a complete orthogonal set is obtained with α restricted to the first $N \times N$ sub-grid of the phase space but it is necessary to define $W(\alpha)$ in a grid of $2N \times 2N$ points for P3 to hold^{13,14}). One can expand the state ρ in terms of this set as $\rho = N \sum_{\alpha} W(\alpha)A(\alpha)$. The coefficients of the expansion are the Wigner function of ρ .

Every time one runs this algorithm with $U = A(\alpha)$ a direct measurement of $W(\alpha)$ is obtained (for any given α). Before presenting results of such measurement for a simple system, it is worth mentioning that the same scheme can be used to measure $W(\alpha)$ in more general cases. For a continuous system $W(\alpha)$ is defined as the expectation value of $A(\alpha) = D^\dagger(\alpha)RD(\alpha)/\pi\hbar$ where $D(\alpha)$ is the phase space displacement operator $D(\alpha) = \exp(i(p\hat{Q} - q\hat{P})/\hbar)$. Therefore, to measure $W(\alpha)$ we need to run the algorithm with the system in the state $D(\alpha)\rho D^\dagger(\alpha)$ (obtained simply by displacing ρ) and use $U = R$.¹⁵ Measuring directly the Wigner function has been the goal of a series of experiments in various areas of physics (all dealing with continuous systems¹⁶). It is remarkable that our measurement scheme describes the recent experiment that determined $W(\alpha)$ for the electromagnetic field in a cavity QED setup.^{17,18} In this case the system is the mode of the field stored in a high- Q cavity and the ancillary qubit is a two level atom. The measurement of the Wigner function is done via a scattering experiment that directly follows the steps described in Figure 1: i) The atom goes through a Ramsey zone that has the effect of implementing an Hadamard transform. An r.f. source is connected to the cavity displacing the field (by an amount parametrized by α) and preparing the state $D(\alpha)\rho D^\dagger(\alpha)$; ii) The atom goes through the cavity interacting dispersively with the field in such a way that only if the atom is in state $|e\rangle$ does it acquire a phase shift of π per each photon in the cavity

(i.e., this interaction is a controlled- $\exp(-i\pi\hat{N})$ gate, where \hat{N} is the photon number, which is nothing but a controlled reflection). iii) The atom leaves the cavity entering a new Ramsey zone and is finally detected in a counter either in the $|g\rangle$ or $|e\rangle$ state. The Wigner function is measured as the difference between both probabilities: $W(q, p) = 2(P(e) - P(g))/\hbar$. As we see, this cavity-QED experiment is a concrete realization of the general tomographic scheme described above.

For a system with a finite dimensional Hilbert space the algorithm can be efficiently decomposed as a sequence of elementary steps: All controlled- \tilde{U} , \tilde{V} and R operations can be implemented via efficient networks like the ones shown in [19] which require a $\text{Poly}(\log(N))$ number of elementary gates. For small N these networks are very simple. We implemented the measurement of $W(\alpha)$ for $N = 4$ (two qubits) for a variety of initial states. In this case R is a controlled not (CNOT) gate (where the control is in the least significant qubit). \tilde{U} is the same CNOT followed by a bit flip in the control. Analogously, \tilde{V} is a sequence of controlled phase gates. The complete circuit has at most one Toffoli gate and several two qubit gates. Figure 3 shows the results of the measurement of the Wigner function for all four computational states of a two qubit system. Ideally, $W(\alpha)$ for the state $|q_0\rangle$ is nonzero only on the vertical strip at $q = 2q_0$, where it is equal to $1/2N$ and on the strip at $q = 2q_0 \pm N$ where it oscillates as $(-1)^p/2N$. These oscillations correspond to interference between the state and its mirror image created by the periodic boundary conditions.¹³

To measure $W(\alpha)$ we used a liquid sample of trichloroethylene dissolved in chloroform. This molecule has been used in several three qubit experiments where the proton (^1H) and two strongly coupled ^{13}C nuclei (C_1 and C_2) store the three qubits.²⁰ We used C_1 as our probe particle and the pair $H-C_2$ to store the state whose Wigner function we measure. The coupling constants are $J_{HC_1} = 200.76$ Hz, $J_{HC_2} = 9.12$ Hz and $J_{C_1C_2} = 103.06$ Hz while the C_1-C_2 chemical shift is $\delta_{C_1C_2} = 908.88$ Hz. We determined the value of $W(\alpha)$ for each of the independent 16 phase space points. Each of these circuits corresponds to a different sequence of r.f. pulses and delays (the number of pulses in each sequence depends on α varying between 5–17 and taking at most 100ms to execute, $\ll T_1, T_2$ of our sample). We used temporal averaging²¹ to obtain, from the part of ρ that deviates from the identity, the four pseudo-pure initial states whose Wigner functions are shown in Figure 3. The experiments were done at room temperature on a standard 500Mhz NMR spectrometer (Bruker AM-500 at LANAIS in Buenos Aires and DRX-500 at Los Alamos). We used a 5mm probe tuned to ^{13}C and ^1H frequencies of 125.77 MHz and 500.13 Mhz. The most important sources of errors come from the strong coupling and the numerical uncertainty in integrating the spectra. These results

illustrate the tomographic measurement of a discrete Wigner function and agree very well with theoretical expectation.

In summary, we presented a general algorithm enabling us to view spectroscopy and tomography as dual tasks. From our algorithm follows the construction of circuits characterizing spectral properties of general operators and the design of a general tomographer with which we can directly measure the Wigner function of the state of a quantum system. The measurement strategy is an example of a very general tomographic scheme in terms of which one can interpret previous experiments performed to measure Wigner functions. The analogy between this quantum computation and a scattering experiment (that has the dual use of providing information either about the state of the scatterer or about the interaction Hamiltonian) is, we believe, particularly illuminating and useful.

References

- [1] D. T. Smithey, M. Beck, M. G. Reymer and A. Farydani, Phys. Rev. Lett. **70** (1988) 1244, G. Breitenbach et al, J. Opt. Soc. Am. **B12** (1995) 2304.
- [2] I. Chuang and M. Nielsen, *Quantum information and computation*, Cambridge Univ. Press (2000).
- [3] A. Yu. Kitaev, Quantum measurements and the Abelian Stabilizer Problem, quant-ph/9511026
- [4] R. Cleve, A. Ekert, C. Macchiavello and M. Mosca, Proc. Roy. Soc. Lond. A **454** (1998), 339
- [5] D. Abraham and S. Lloyd, Phys. Rev. Lett. **83** (1999), 5162-5165.
- [6] E. Knill and R. Laflamme, Phys. Rev. Lett. **81** (1999), 5672.
- [7] R. Laflamme, J. P. Paz and M. Saraceno, in progress.
- [8] G. Ortiz, J. E. Gubernatis, E. Knill and R. Laflamme, Phys. Rev. A **64** (2001) 022319/1–14; R. Somma, G. Ortiz, J.E. Gubernatis, R. Laflamme and E. Knill, *in preparation*
- [9] O. W. Sørensen and G. W. Eich and M. H. Levitt and G. Bodenhausen and R. R. Ernst, Prog. NMR **16** (1983) 163–192.

- [10] D. G. Cory *et al*, Fortschritte der Physik special issue, Experimental Proposals for Quantum Computation **48** (2000) 875-907.
- [11] M. Hillery, R. F. O'Connell, M. O. Scully, E. P. Wigner, Phys. Rep. **106** (1984), 121.
- [12] J. P. Paz and W. H. Zurek, in “*Coherent matter waves, Les Houches Session LXXII*”, edited by R Kaiser, C Westbrook and F David, EDP Sciences, Springer Verlag (Berlin) (2001) 533-614.
- [13] P. Bianucci, C. Miquel, J. P. Paz and M. Saraceno, quant-ph/0106091, (2001) submitted to PRL; C. Miquel, J. P. Paz and M. Saraceno in preparation.
- [14] J. H. Hannay, M. V. Berry, Physica **1D** (1980), 267; A. Rivas, A. M. Ozorio de Almeida, Ann.Phys. **276** (1999), 123
- [15] To measure the continuous Wigner function one can choose between two equivalent options: i) applying the circuit of Figure 1 with $U = D(\alpha)RD^\dagger(\alpha)$, or ii) apply first the operator $D(\alpha)$ displacing the initial state ρ and later use the circuit with $U = R$. This later option is more convenient since in this way the only operation that needs to be controlled by the ancillary qbit is the reflection R (this is precisely what is done in the cavity QED experiment described in the text). This strategy can always be applied for operators of the form $U = GBG^\dagger$ (in such case, one can first unconditionally apply the operator G to the initial state and later use a simpler circuit with $U = B$). It is interesting to notice that this strategy can be applied to the measurement of the discrete Wigner function only if both q and p are even (some of these peculiar features of discrete Wigner functions are discussed in [13]).
- [16] T. J. Dunn *et al.*, Phys. Rev. Lett. **74** (1994) 884; D. Leibfried *et al.* Phys. Rev. Lett. **77** (1996) 4281; see also Physics Today **51** no. 4 (1998) 22; L. Lvovsky *et al.* Phys. Rev. Lett. **8705** (2001) 050402.
- [17] L. G. Lutterbach and L. Davidovich, Phys. Rev. Lett. **78** (1997) 2547; Optics Express **3** (1998) 147.
- [18] G. Nogues *et al*, Phys. Rev. **A** (2000); see also X. Maitre *et al*, Phys. Rev. Lett. **79** (1997) 769.
- [19] C. Miquel, J. P. Paz and R. Perazzo, Phys. Rev. **A54** (1996), 2605.
- [20] see for example: M. A. Nielsen, E. Knill, R. Laflamme, Nature **396** (1998), 52–55; D. G. Cory *et al.*, Phys. Rev. Lett. **81** (1998) 2152

[21] E. Knill, I. Chuang, and R. Laflamme, Phys. Rev. **A57** (1998) 3348–3363.

Figure 1: Circuit for measuring $\text{Re}[\text{Tr}(\rho U)]$, for any unitary operator U .

Figure 2: Circuit for evaluating the spectral density of an operator U . The second register, formed by n_1 qubits, is prepared in the initial state $|E\rangle$ and is subject to a controlled Fourier transform. The second controlled operator acts on the second and third registers mapping the computational states $|t\rangle_2 \otimes |n\rangle_3$ into $|t\rangle_2 \otimes U^t|n\rangle_3$.

Figure 3: Measured Wigner functions for the four computational states of a two-qubit system (built with a liquid sample of TCE in an NMR spectrometer). Ideally, these Wigner functions should be nonzero only on two vertical strips where they take values which are $\pm 1/8$. Experimental results show small deviations from these values (with a maximum error of 15%).

Figure 1. Juan Pablo Paz <paz@df.uba.ar>

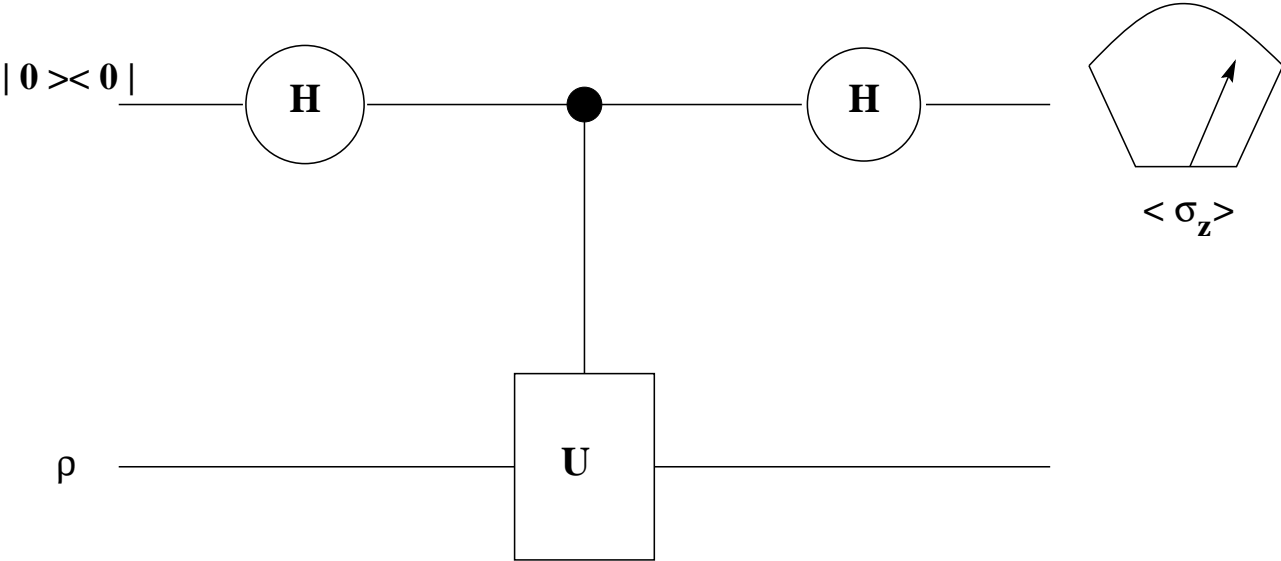


Figure 2. Juan Pablo Paz <paz@df.uba.ar>

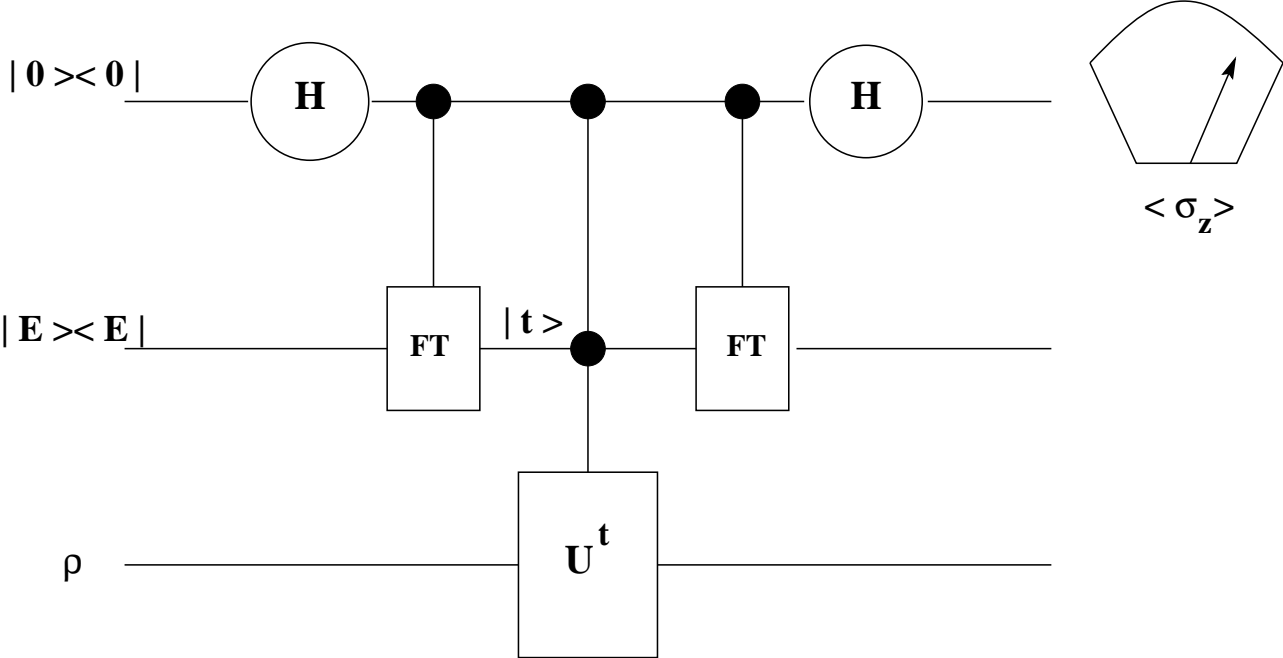


Figure 3. Juan Pablo Paz <paz@df.uba.ar>

